

# The characteristics of cavity mode in trilayer Dielectric/Metal/Dielectric plasmonic thermal emitter

Yu-Wei Jiang, Dah-Ching Tzuang, Yi-Ting Wu, Ming-Wei Tsai, and Si-Chen Lee\*

Graduate Institute of Electronics Engineering, Department of Electrical Engineering,  
National Taiwan University, Taiwan  
phone: +886-2-33663700 #440; E-mail: sclee@ntu.edu.tw).

**Abstract-** A suitable designed trilayer Ag/SiO<sub>2</sub>/Au thermal emitter can be used as the narrow bandwidth infrared light source. The thermal radiation generated in the SiO<sub>2</sub> layer resonates between the two metal films and results in not only the Ag/SiO<sub>2</sub> surface plasmon polaritons but also the cavity mode in the Ag/SiO<sub>2</sub>/Au waveguide. The interaction between surface plasmon polaritons and the cavity modes was investigated, and the theoretical dispersion relation was derived which fitted well with the experimental results. This cavity mode light source can be applied in the area of gas sensing and probing the response of the animal cells and plants to the infrared radiation.

## 1. Introduction

Surface plasmon polaritons (SPPs) are electromagnetic excitations, propagating along a dielectric/metal interface and having the electric field components perpendicular to the surface decaying exponentially into both neighboring media [1]. The trilayer metal/dielectric/metal structure can support spatial light confinement due to coupling with SPPs, with no light diffraction limitation, at both metal/dielectric interfaces [2]. The coupling mechanism changing from SP to Fabry-Perot resonance as a function of dielectric material thickness are investigated that the strong interaction results in the formation of a waveguide-plasmon polariton [3]. In this letter, the ultra-narrow bandwidth cavity modes in Ag/SiO<sub>2</sub>/Au plasmonic thermal emitters are demonstrated. The emission spectra and dispersion relations are characterized with respect to the SiO<sub>2</sub> layer thickness, and the coupling mechanism between cavity and surface plasmons modes are investigated.

## 2. Experiments and results

A 400 nm thick Mo films was thermally deposited on the back of the double-polished Si substrate as a heating source. A 20 nm Ti and 200 nm Au metal film were deposited on the front side of the Si substrate followed by a SiO<sub>2</sub> layer deposited with the plasma enhanced chemical vapor deposition (PECVD). The thicknesses of the SiO<sub>2</sub> layer in devices A to E were 0.7, 1.1, 1.6, 2.1, and 2.6  $\mu\text{m}$ , respectively. Then a 100 nm-thick silver film was deposited and lifted-off on SiO<sub>2</sub> layer to form hexagonal holes arrays with lattice constant of 3  $\mu\text{m}$  and holes diameter of 1.5  $\mu\text{m}$ . The radiation area of the sample was 1  $\text{cm}^2$ . The schematic diagrams showing the side and top views of the device structure are depicted in Figs. 1 (a) and (b), respectively. A Bruker IFS 66 v/s system was used to measure reflection spectra. The sample was defined to lie in the (x, y) plane rotating around the y axis in 1° increments from  $\theta=12^\circ$  to

$\theta=65^\circ$ . The light was incident in the z direction, allowing the dispersion relation in the  $k_x$  ( $\Gamma\text{K}$ ) direction to be measured. A PERKIN ELMER 2000 Fourier Transform Infrared Spectrometer (FTIR) system was adopted to measure the thermal radiation spectra. A DC current was sent into the back Mo metal on Si substrate to heat the sample, the thermal couple was put on the top of the sample to measure the temperature. Fig. 2 (a) to (d) shown the energy dispersion relations as a function of  $\vec{k}_x$  for devices A, B, C, and D with various SiO<sub>2</sub> thicknesses, i.e., 0.7, 1.1, and 2.6  $\mu\text{m}$ , respectively. For device A with SiO<sub>2</sub> thickness of 0.7  $\mu\text{m}$ , four dark lines representing the reflection minimum and the excitation of SPPs intersect with y axis at 0.32 eV ( $\sim 3.88 \mu\text{m}$ ) that is composed of six degenerate modes, i.e.,  $(\pm 1, 0)$ ,  $(0, \pm 1)$ ,  $(-1, 1)$  and  $(1, -1)$  Ag/SiO<sub>2</sub> modes denoted as  $(1, 0)$  Ag/SiO<sub>2</sub> mode. The dark area at the higher energy represents the intense absorption band. The absorption band narrowed and shifted to lower photon energy, blending with  $(+1, 0)$  Ag/SiO<sub>2</sub> mode with increasing SiO<sub>2</sub> thickness from 0.8 to 0.9  $\mu\text{m}$  (not shown). When the SiO<sub>2</sub> thickness exceeded 1.1  $\mu\text{m}$  as shown in Fig. 2 (b), the cavity mode appeared and mixed with Ag/SiO<sub>2</sub> mode, it could be considered as a F-P type resonance generated in SiO<sub>2</sub> layer between two parallel metal planes. In particular, the dispersion curves shown in Fig. 2 (b) displayed the anti-crossing like behavior of the two modes around 0.35 eV, which was attributed to the coupling

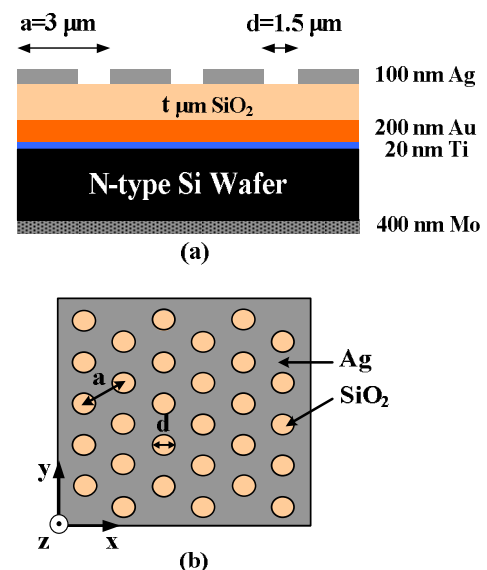


Fig. 1 Schematic diagram of the (a) side and (b) top view of the Ag/SiO<sub>2</sub>/Au plasmonic thermal emitter, the top metal is perforated with hexagonal hole array.

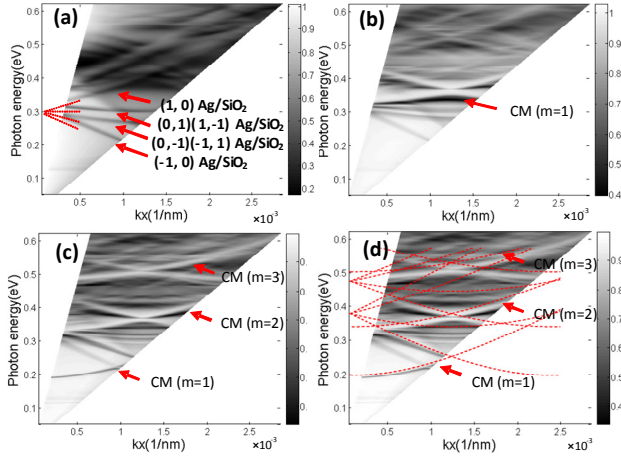


Fig. 2 Measured energy dispersion relation as a function of  $\bar{k}_x$  along  $\Gamma K$  direction for devices A, B, and E with different SiO<sub>2</sub> thicknesses  $t$  of (a) 0.7  $\mu\text{m}$ , (b) 1.1  $\mu\text{m}$ , and (c) 2.6  $\mu\text{m}$ . The theoretical energy dispersion relation (red lines) are shown to fit the experimental result of (d).

between the propagating waves and its diffractive waves by Brillouin zone boundary in momentum space. From the theoretical calculations, the cavity mode with momentum  $k_{gw}$  is given by

$$k_{wg} = k_x + iG_x + jG_y \quad (1)$$

here  $k_x = \omega \sin \theta / c$ ,  $G_x$  and  $G_y$  are the reciprocal lattice vectors associated with the hexagonal array,  $\omega$  is the incident photon frequency,  $\theta$  is the incident angle,  $c$  is the light velocity. For parallel plate waveguide, the dispersion relation is given by

$$k_{wg} = \left[ \left( \frac{\omega}{c} \times n \right)^2 - \left( \frac{m\pi}{t} \right)^2 \right]^{1/2} \quad (2)$$

where  $m$  is the mode number,  $n$  and  $t$  are the refractive index and thickness of SiO<sub>2</sub> layer, respectively. By solving the Eqs. (1) and (2), the calculated dispersion curves (dotted red lines) are shown in Fig. 2 (d), they appear in good agreement with the experimental results. Besides, the higher energy (shorter wavelength) zone shown the slight redshift, comparing with the calculated result. It is because at higher photon energy, the cavity mode becomes easier to leak out the top metal hole array that leads to an increase of effective SiO<sub>2</sub> layer thickness.

The emission spectra of devices B, C, D, and E with increasing SiO<sub>2</sub> thickness, i.e., 1.1, 1.6, 2.1, and 2.6  $\mu\text{m}$ , were measured at normal incidence and displayed in Fig. 3 (a), (b), (c) and (d), respectively. In Fig. 3 (a), the peak at 4.11  $\mu\text{m}$  is a mixed mode, composing of Ag/SiO<sub>2</sub> SP and fundamental ( $m=1$ ) cavity mode (CM). The small shoulder at 3.86  $\mu\text{m}$  ( $\sim 0.32$  eV) is the Ag/SiO<sub>2</sub> SP mode which can be seen as the mixing modes in Fig. 2 (d). The peak at 3.08  $\mu\text{m}$  is a cavity-grating coupled mode composed of six degenerate modes, i.e.,  $(\pm 1, 0)$ ,  $(0, \pm 1)$ ,  $(-1, 1)$  and  $(1, -1)$  modes denoted as  $(1, 0, m=1)$  cavity mode. The peak positions of the fundamental cavity mode ( $m=1$ ) are found to redshift with increasing SiO<sub>2</sub> thickness; however, the peak position at 3.86  $\mu\text{m}$  associated with  $(1, 0)$  Ag/SiO<sub>2</sub> modes remain fixed when SiO<sub>2</sub> thickness exceed 1.1  $\mu\text{m}$

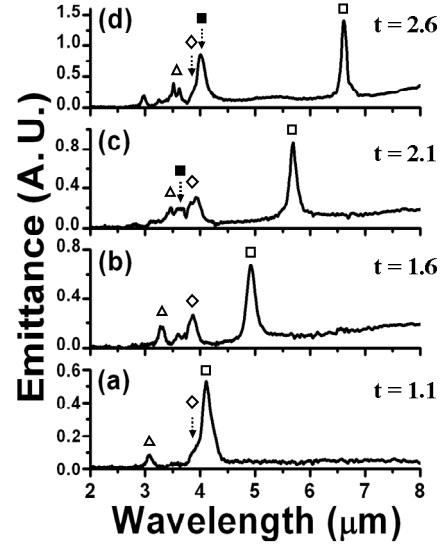


Fig. 3 Measured emission spectra of device B, C, D, and E with different SiO<sub>2</sub> layer thicknesses, i.e.,  $t =$  (a) 1.1, (b) 1.6, (c) 2.1, and (d) 2.6  $\mu\text{m}$ , respectively. The spectra show fundamental cavity mode ( $m=1$ ) (open square),  $(1, 0)$  Ag/SiO<sub>2</sub> SPP mode (open diamond), second order cavity mode ( $m=2$ ) (solid square), and  $(1, 0, m=1)$  cavity mode (open triangle). The devices with lattice constant  $a = 3$   $\mu\text{m}$  and diameter  $d = 1.5$   $\mu\text{m}$  was heated at fixed temperature of 140  $^{\circ}\text{C}$ .

resulted from the weak coupling between top and bottom Ag/SiO<sub>2</sub> modes. From emittance spectra displayed in Fig. 3 (b), the 4.92  $\mu\text{m}$  peak, which is a fundamental cavity mode, exhibiting stronger intensity between two metal slabs than that of SP. The peak at 3.3  $\mu\text{m}$  with regard to  $(1, 0, m=1)$  cavity mode, which follow the fundamental cavity mode, showing the redshift with increasing SiO<sub>2</sub> thickness. The peak at 3.65  $\mu\text{m}$  depicted in Fig. 3 (c) is a second-order cavity mode ( $m=2$ ), which shift to 4.01  $\mu\text{m}$  and mix with Ag/SiO<sub>2</sub> mode at 3.86  $\mu\text{m}$  when SiO<sub>2</sub> thickness is 2.6  $\mu\text{m}$ , shown in Fig. 3 (d). The ratio  $(\Delta\lambda/\lambda)$  of the FWHM to the peak wavelength for fundamental cavity mode in the devices E, F, G are 0.20, 0.158, and 0.118  $\mu\text{m}$ , respectively, demonstrating the property of narrow bandwidth cavity mode is better than that of SP [3].

### 3. Conclusion

In conclusion, the ultra-narrow bandwidth Ag/SiO<sub>2</sub>/Au infrared thermal emitters were fabricated successfully. As the SiO<sub>2</sub> layer is thin, the Ag/SiO<sub>2</sub> SPPs modes are clearly seen. While the SiO<sub>2</sub> layer becomes thicker than 1.1  $\mu\text{m}$ , cavity mode determined by waveguide-cavity cut-off frequency appears on the emission spectra. The interaction between the cavity and SPP modes was investigated. The theoretical calculation shows a good agreement with the experimental results.

### References

1. H. Raether, Surface Plasmons (Springer-Verlag, Berlin, 1988).
2. J. A. Dionne, H. J. Lezec, and Harry A. Atwater, "Highly Confined Photon Transport in Subwavelength Metallic Slot Waveguides" Nano Lett. 6, (2006), pp.1928-1932.
3. A. Christ, S. G. Tikhodeev, N. A. Gippius, J. Kuhl, and H. Giessen, "Waveguide-Plasmon Polaritons: Strong Coupling of Photonic and Electronic Resonances in a Metallic Photonic Crystal Slab" Phys. Rev. Lett. 91, (2003), pp.183901-183904.